



Fabrication of nano-adsorbent and its kinetics studies for sorption of textile reactive dye

K.V. Radha*, V. Gopalakrishnan and B. Vijayalakshmi

Bioproducts Laboratory, Department of Chemical Engineering, A.C.Tech., Anna University, Chennai 600025, India
radhavel@yahoo.com

Available online at: www.isca.in, www.isca.me

Received 10th June 2020, revised 9th October 2020, accepted 5th December 2020

Abstract

The present study details on the synthesis of Silver nanoparticles using the leaves of *Tamarindus indica* for application as dye removal agent as a first attempt. Effort has been made using the obtained nanomaterial for environmental applications as bio sorbent. Characterization of the obtained nanoparticles was done using X-Ray Diffraction Spectrometer (XRD), Fourier Transform Infra-Red Spectrometer (FTIR) and Raman spectroscopy. The novel nanomaterial resulted from the synthesis had organic surface molecules due to the phyco-chemicals that was confirmed through FTIR. The incorporation of the phyco-chemicals was identified from the X-ray diffraction patterns of silver nano particles. The morphology of the nanoparticles as observed from SEM was found to be smooth, spherical, and homogeneously distributed of size around 20 nm, also confirmed through TEM. Adsorption studies using the nano sorbent showed significant dye reduction of 97.4% at optimum conditions of 7.0 pH at 27°C with 300 mg of Silver nano particles. Kinetic studies on adsorption were carried out, which showed pseudo second order kinetics fits well the adsorption studies with favourable adsorption of reactive dye used. The obtained nanomaterial can be instantly used for controlling the dye that is polluting the environment from textile industries.

Keywords: Silver nano particles; *Tamarindus indica*; reactive dye; adsorption; kinetics.

Introduction

Drinking water is decisive for human being, and apart from drinking to survive, mankind needs pure water for cooking, cleaning, washing etc. Industrialization, causes most of the water in the industries to release polluted water into the environment¹. One among the major industries that pollute the water bodies are the textile industries. The major cause of the detergent effect in environment from textile industries is due to the dyes used on cloth materials². As new fashion arises, the need for different dye colours with persistent distinctive sheen is need of the hour³.

Synthetic dyes pose a threat to health and environment as they cause toxicity and have adverse effect on living beings⁴. Therefore, research is being made to remove these pollutants. Physical and chemical methods are used for treatment purposes⁵. The eco-friendliness and cost effectiveness make the biological treatment to overcome the above-mentioned methods.

Recently nanoparticles have come into existence for treating pollution of any cause, owing to their outstanding ability to endure adverse processing conditions as compared to other methods. Biosynthesized nanoparticles have significant advantages in applications such as biomedical^{6,7} and environmental⁸. The biological method of synthesis of nano size materials gives better biocompatible nanoparticles⁹. Silver nanoparticles are synthesized using different approaches namely chemical, electrochemical, microwave, sol-gel techniques,

precipitation and biological synthesis. Nanoparticles are obtained with divergent properties that include surface area, size, shape etc., but green synthesis is the highly prevalent recently due to its cost factor and time consumption. Another major advantage is it can be synthesized by altering the proportions of the extracts as to the need of the nanomaterial.

Adsorption process suits well to remove organic matter from waste effluents and credit goes for its applicability in terms of cheap technology. Moreover, the technique is cost effective and directness in design. Hence it can be easily operated^{10,11}. It does not produce any harmful secondary pollutants during decontamination. In adsorption process, solid adsorbents are widely employed to eradicate definite class of pollutants, from wastewaters; especially those which are not separated by conventional treatment methods. A conventional method for treatment of wastewater and industry effluents must satisfy the environmental, social and economic requirements and is then being considered as a sustainable end-of-pipe technology¹².

The focal point of the current study is to synthesize the silver nanoparticles using a greener route using the leaves of the plant, *Tamarindus indica* and to use the prepared nanomaterial for dye removal. Biosynthesis of silver nanoparticles (AgNPs) is made through novel attempt of using leaves of the plant *Tamarindus indica*, as this plant is mainly used for medical application as such. The *Tamarindus indica* leaf extracts was used to reduce metal ions, which are voluntarily scalable and nontoxic

compared to that of physical and chemical treatment methods¹³. The formation of the nanomaterial was characterized using instrumental analysis such as Scanning Electron microscopy (SEM) for structural clarification, Transmission electron microscopy (TEM) for size analysis, X-ray diffraction (XRD) and Fourier Transform Infrared spectrometer (FTIR) for crystallinity and chemical composition analysis. The thermal stability was checked by Thermo gravimetric and differential thermal analysis (TG-DTA). The initial dye concentration, optimum conditions including pH, temperature concentrations of nanomaterial were tested and optimized. Studies were conducted to check the detoxification of wastewater after treatment with Silver nanoparticles, sorption studies with kinetics were carried out for the dye removal.

Materials and methods

Chemicals: Silver nitrate, potassium phosphate monobasic, dihydrogen potassium orthophosphate was bought from Sisco Research Laboratories, Mumbai, India and Reactive Brilliant Blue R from Textile Department of Anna University, India. All chemicals used in this work were seen to be of analytical grade and used as such obtained. All solution preparations were made with distilled water.

Preparation of Plant Extract: The plant was thoroughly washed with running water. Washed again well with double distilled water, air dried at room temperature for upto two hours. The material was now cut into tiny pieces. This was again treated for moisture by drying in room temperature for seven days. After testing for the dryness the moisture relived leaves were ground to powder form. The material was filtered through fine sieve for fineness and ground again which was stored at room temperature. The powder (5g) was weighed and mixed in 100 ml of double distilled water. This was allowed to percolate within the water for about 24 hours maintaining at 37°C. The Plant extract was filtered through Whatman filter paper no 1 to get a clear filtrate¹⁴.

Silver Nanoparticles synthesis: About 10 mg of *Tamarindus indica* leaf was taken and made into aqueous extract. About 90 ml of 1 mM silver nitrate solution was taken along with and mixed using a magnetic stirrer for 2 hours at 37°C. Initially the color of the solution was yellow and now the colour changed to bright brownish color. This is the indication of the size reduction; the formation of silver nanoparticles (AgNPs). The formation of Agnps is due to the aqueous silver ions reduction by aqueous extract of leaves to produce firm silver nanoparticles in solution¹⁵. After some time Agnps were removed through centrifugation. To remove the possible impurities in the sample, it was washed with acetone. To get a pure sample it was washed again and again. Drying of the obtained nanopartcles was carried out for necessary hours to remove moisture content and then the nano powders were collected and stored in airtight containers.

Silver Nanoparticles Characterization: The synthesized Silver nanoparticles were characterized using T90+ UV-Vis

spectrophotometer, PG instrument Ltd. in the wavelength range of 400-500nm to confirm the formation of silver nanoparticles that were obtained from silver ions using plant extract¹⁶.

Scanning Electron Microscopy (SEM) was performed with TESCAN VEGA3 SBU to study the surface morphology of silver nanoparticles initially and then the coated filter was studied for changes in structure of the nanoparticles¹⁷.

Energy dispersive X-ray spectroscopy using a Bruker X-flash detector with the energy of the electron beam maintained at 15 keV¹⁸ was used to find the elements and its composition of the silver nanoparticles

Transmission Electron Microscopy Analysis (TEM) was done to understand the morphology and particle size distribution of silver nanoparticles. The grid for TEM analysis was prepared by placing a drop of the sample suspension on a carbon-coated copper grid and analyzed under a Jeol 3010 TEM at 200 KV.

Fourier Transform Infrared spectroscopy (FTIR) was done using Jasco FTIR 6600 to find the functional groups of plant extract accountable for lessening and stabilization of AgNPs. Raman spectra of the particles were obtained using Horiba Jobin Yvon Lab RAM HR micro Raman system¹⁹.

X-ray diffraction of biosynthesized silver nanoparticles were done on a CuK α 1. The particle size and nature of silver nanoparticle was determined using X-Ray Diffraction²⁰.

Adsorption kinetics and isotherms: Reactive Brilliant Blue R dye was used for adsorption and kinetic studies along with the synthesized Silver nanoparticles²¹. A stockpile solution of 1000 mg/L of the dye was prepared in distilled water. The stock solution was diluted to obtain the working solutions containing 10-50mg/L of the dye concentrations. Batch adsorption studies were performed using 50mL conical flask containing 10mL of the dye solution. The different adsorption conditions such as, initial pH (3-9), initial concentration (10-50mg/L), adsorbent dosage (10-500mg) and contact time (0-240min) were investigated in a mechanical shaker at constant room temperature.

The experiments used to determine the effect of pH were performed using 100mg of silver nanoparticles in 20mL of 10mg/L of the Reactive Brilliant Blue R dye solution at various pH ranges, adsorbent dosages²². The studies were categorically done for one hour. At the end centrifugation was done at 10,000 rpm for 30min. The supernatant was taken for analysis. UV-Vis spectrophotometer was used to analyze the tested samples at 592nm. Percentage adsorption calculations were based on conventional techniques²³.

Analysis of Data: All measurements were repeated three times except analytical instrumental analysis. Microsoft Excel 2010 was used for Statistical analysis with an accepted significance level (α) as 0.05.

The results represented as $X \pm \Delta X$, where X is the average value and ΔX is standard deviation.

Results and discussion

Synthesis of Silver nanoparticles: On addition of *Tamarindus indica* leaf extract to aqueous silver nitrate solution, change in yellow to yellowish-brown colour was observed after about 2 h of reaction. This is the indication of formation of silver nanoparticles²⁴. The reduction of Ag^{2+} ions is confirmed by visible colour change in the reaction mixture. Analysis on UV-Vis spectrophotometer (Figure-1) shows the Phyto stabilized silver nanoparticles has maximum absorption peak at 430nm, proves silver nanoparticles formation. Siddiqi et al.,²⁵ have predicted the absorption peak at 420-460nm for stabilized silver nanoparticles formation. These results coincide well with our own result, which indicates the formation of stable reduced Agnps. A clear confirmation was obtained further with literature survey for making green synthesized silver nanoparticles.

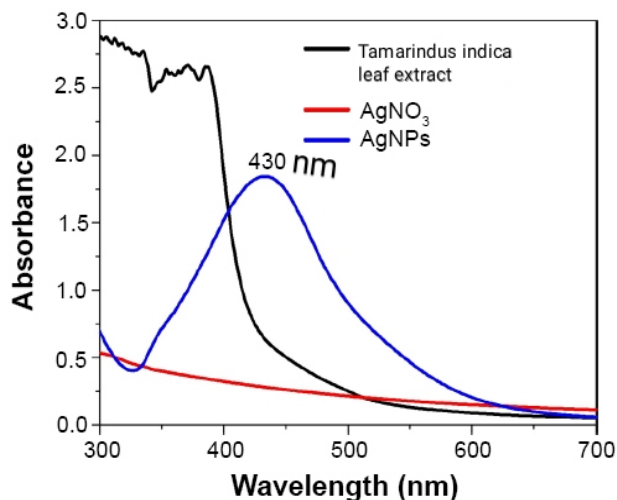


Figure-1: UV visible spectra of (a) plant extract, (b) 1mM Silver nitrate and (c) Silver nanoparticles.

Characterization Studies: X-ray Diffraction studies: X-ray Diffractometer was used to study the purity of the materials, whether it is crystalline and have phase purity and about the particles nature. For this the X-ray source was $CuK\alpha.1$ Figure-2 represents the XRD pattern of the obtained nanoparticles. The peak intensities match with the standard (JCPDS NO: 87-0720) indicating that the synthesized nanoparticles in absence of any roughness. Peaks were observed at 2θ in the diffraction studies. They were at 38.048° , 44.49° , 64.61° and 77.53° corresponding to (111), (200), (222), and (311) planes, respectively. These peaks agree very well with the standard. Thus it can be clearly stated for Ag FCC arrangement. The results conclude that the silver nanoparticle formed using *Tamarindus indicaleaf* extract is purely crystalline in nature. Moreover, the particles show single phase. No other definite diffraction peaks were observed. The peak obtained truly represents characteristic Ag phase.

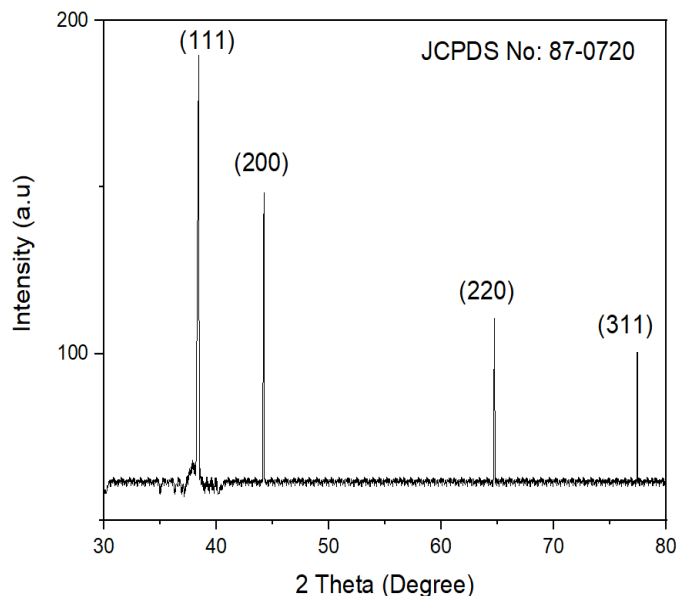


Figure-2: XRD spectrum of Silver nanoparticles.

Debye-Scherrer formula was used for calculating d spacing. Bragg's equation and the average crystallite size was found out using the Debye-Scherrer formula, Bragg' law for d-spacing calculation formula is

$$d = \frac{n\lambda}{2\sin\theta}$$

Where, d is the inter planar distance, n is the order of diffraction whose value is 1 for first order diffraction, λ is the wave length of the X-Ray (1.54 \AA for $CuK\alpha.1$) and θ is the diffraction angle From the full width at half maximum, the grain size for the sample can be calculated from half widths of the major diffraction peak (111) according to Debye-Scherrer formula,

$$\tau = \frac{K\lambda}{\beta \cos\theta}$$

Where τ is the crystallite size, K is the shape factor (0.9) and β is the Full Width at Half Maximum (FWHM) in radian, θ is the diffraction angle²⁶. The Average crystallite size was found to be 19.89 nm and the average d-spacing was calculated as 1.342 nm. The results are well coinciding with the TEM image results, thereby consistency in results are well collaborated,

Energy Dispersive X-Ray Analysis (EDX): Energy Dispersive X-Ray Analysis (EDX) demonstrated the presence of the element Ag in Ag-Nps. The image explicitly show clear signal of Ag (Figure-3). Silver nano particles usually indicate standard optical absorption peak approximately at around 3.4 keV²⁷ and the same was obtained in our results. C and O were also obtained meekly which suggest for mixed precipitates that are

present in the plant extract. Many slight but no so clear distinctive peaks might be due to the precipitates as well.

FTIR and SEM Analysis: Surface characteristics of the Silver nanoparticles: The surface properties of the silver nanoparticles were analyzed using FT-IR analysis (Figure-4). From the characteristics peak obtained, one at 3424cm^{-1} indicates OH bending in both plant extract and silver nitrate which shows the coating of Phyto phenolic compounds on the nanoparticles²⁸. Hence it can be inferred that these compounds were involved in the reduction process. In FTIR, the peak reveals the carbonyl bond presence (1740cm^{-1}), aliphatic group (1632cm^{-1}), aromatic ring (1415cm^{-1}) and ester (1075cm^{-1}). The plant extract has the active ingredients such as flavonoids, alkanoids and alkaloids which constitute to act as capping agents. When the size of Silver nitrate particles was reduced to nanosized, the surface bond force constant increased due to the effect of fixed size of nanoparticles. There is a shift in wavelengths from pure to reduced *Tamarindus indica* leaf extract as they were capped by AgNPs. The bands at $1,074$ and $1,042\text{cm}^{-1}$ in the spectra of *Tamarindus indica* leaf extract and AgNPs, respectively, was due to $-\text{C}-\text{C}-$ stretching and it corresponds to the crossing point between silver and *Tamarindus indica* leaf extract.

Surface morphology is characterized using Scanning Electron Microscopy (SEM) for silver nano particles (Figure-5). The figure confirms that the silver nanoparticles are cubic in nature and highly uniform in size. The SEM image showed that the surface of the particles was coarse in nature. These characteristics were mainly because of the agglomeration of the

particles. This can be prevented by homogenizing the particles using mortar and pestle. After homogenization, Transmission electron microscopy (TEM) for the silver nano particles was taken (Figure-6). The TEM analysis revealed the spherical structures of the nanoparticles and it was very well clear that they were homogeneously distributed. Moreover, the nanoparticles were approximately 20nm in size. Surface coatings were also visible in the TEM images which were because of the phycochemicals present in the *Tamarindus indica* leaf extract.

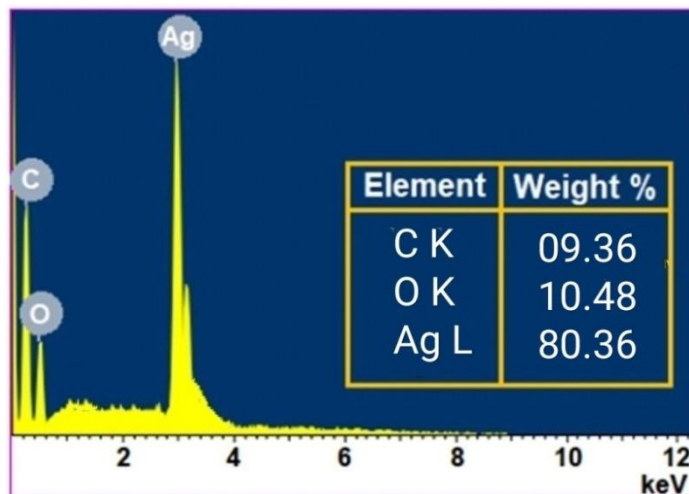


Figure 3: Energy Dispersive X-ray Spectroscopy (EDX) analysis of AgNPs.

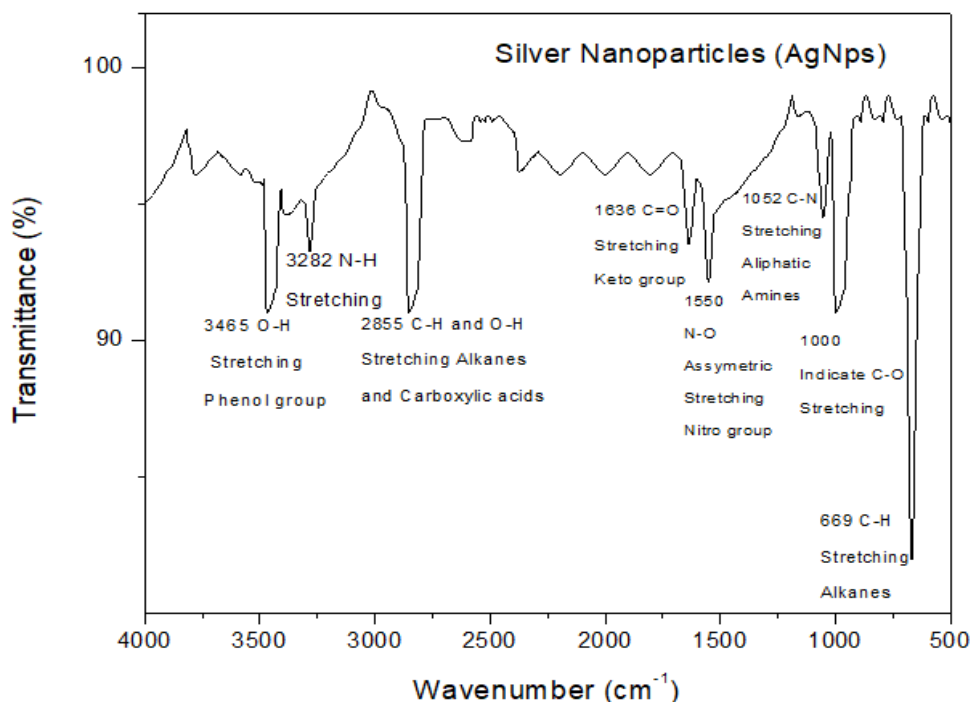


Figure-4: FTIR spectrum of the Silver nanoparticles.

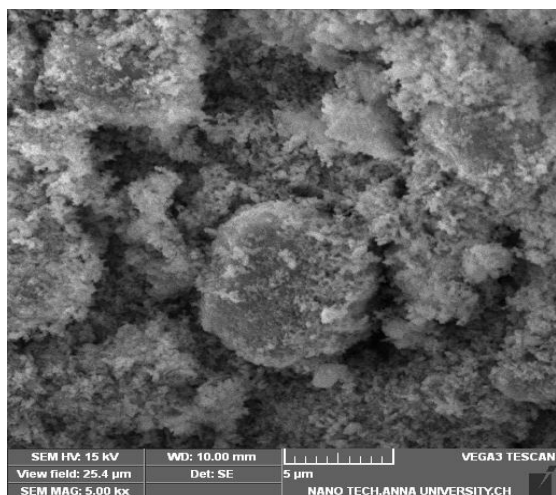


Figure-5: SEM image of the silver nanoparticles.

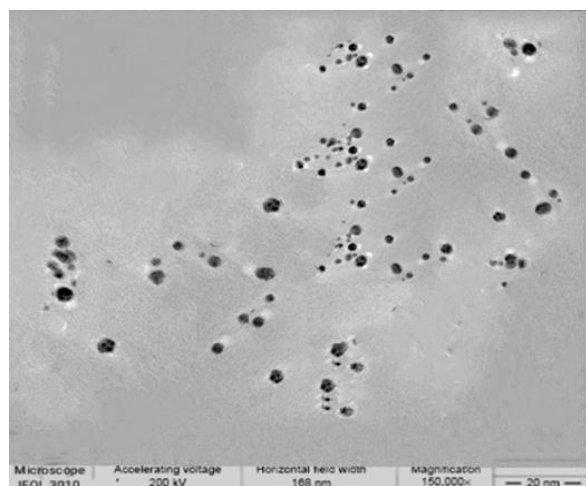


Figure-6: TEM image of the silver nanoparticles.

Studies on Adsorption: Effect of initial pH on dye adsorption: Adsorption studies were done to study the effect of initial pH on the dye, Reactive Brilliant Blue R (20mL) with

100 mg of Silver nanoparticles. The pH of the solution affects greatly the adsorption behavior due to the adsorbate solubility and the ionizing groups present. Dye concentration (20mg/L), adsorbent dosage (0.3g/L), temperature (32⁰C), were maintained for pH studies (Figure-7). The percentage dye removal increased from pH 3 to 7, where there was highest biosorption. When the pH of the solution was increased further, the percentage removal decreased to a larger extent for a value of 51% at 9 pH. Removal of dye, as seen in figure, increased by escalating the pH up to 7.0 and after that the removal efficiency was reduced. This is because at elevated pH the surface of the nanoparticles was altered by -OH groups which made them unsuitable for adsorption of dye. Electrostatic interactions play a major role between positively and negatively charged ions of the adsorbent and the dye solution²⁹. The experimental value either decreases or increases, Higher values than 7, increases the negativity and below 7 positivity of the ions and thereby altering the surface reaction of the Silver nanoparticles. From the results obtained all adsorption experiments were conducted at pH 7.0.

Effect of temperature on adsorption of dye: Temperature dependence on the adsorption efficiency of Reactive Brilliant Blue R (20mL) onto the Silver nanoparticles (300mg) was performed (Figure-8). On observations, the dye uptake capacity increased with mounting temperature up to 27⁰C that indicates the adsorption capacity of the Silver nanoparticles. The temperature was favorable for a temperature from 25⁰C to almost 35⁰C. The long duration adsorption behavior might be due to the kinetic energy increase favored biosorption of the Silver nanoparticles. And one more factor might be the available active sites were available due to the collision rate that occurred at that temperature range. The removal efficiency reduced with further rise in the temperature. At higher temperatures mobility of the particles raises furthermore which in turn increases desorption process. The result can be concluded that the progress might be endothermic. Thus, as the temperature is increased the adsorption efficiency is reduced.

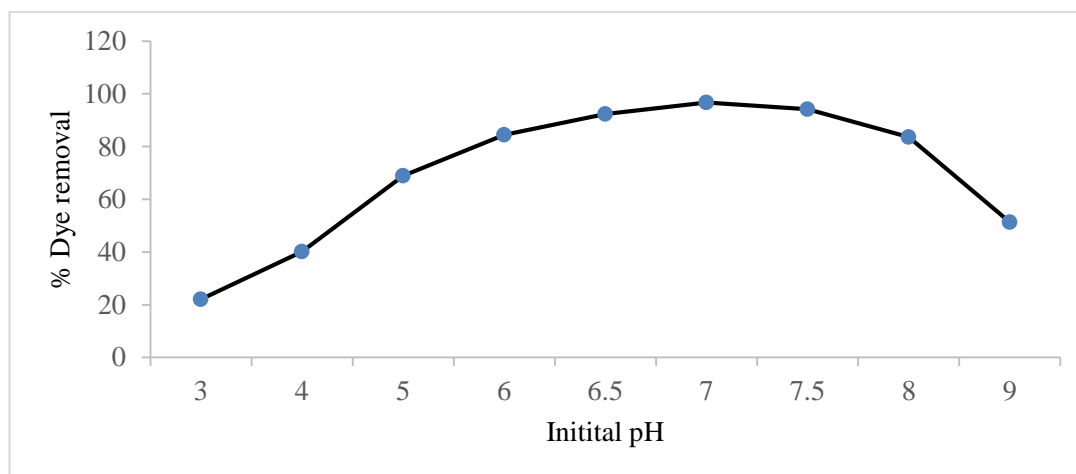


Figure-7: Effect of initial pH on the removal of Reactive Brilliant Blue R.

Adsorbent dosage effect: Biosorption capability represents the bio sorbate content that is retained in the mass of the sorbent. The Reactive navy blue biosorption was examined by changing the dosage from 10 to 50mg at a concentration of 10mg/L in a solution volume of 100mL. The speed of agitation was fixed at 100rpm. Figure-9 shows bio sorbent dosage vs. biosorption capacity and as observed from the results, augment in the mass of bio sorbents led to an augment in removal, from 35.60% to 97.82% However, increasing the dosage beyond 0.35g did not show any major change in adsorption. From 0.3 to 0.5g there was almost saturation with respect to dosage amount and after 0.5mg it caused a decrease in biosorption capacity. Large

number of active sites presents initially with the mass increases the adsorption capacity³⁰. As and when the active sites are filled, and no more active sites present there tends to be a decrease in adsorption behavior. At this time the dye molecules are present in higher concentration even though the mass of the adsorbent remains the same. Particle aggregation also play a major role in decreasing the surface area available due to which diffusion path of the dye gets narrowed down to get into the bio sorbent³¹. Thus in the further experiments 300mg of Silver nanoparticles were included with 20mL of the dye solution to perform the batch adsorption studies.

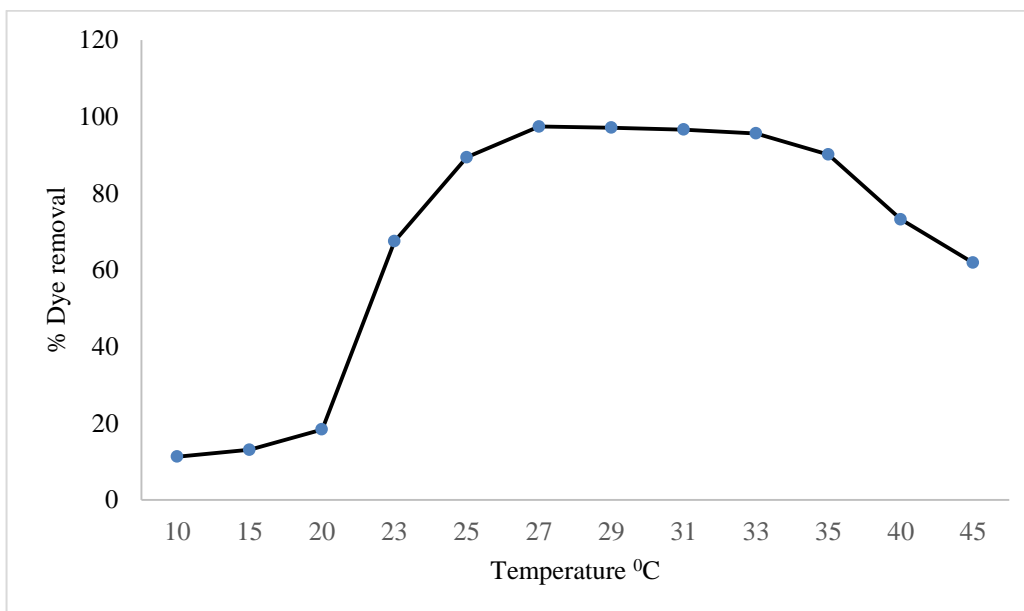


Figure-8: Temperature effect on the adsorption of Reactive Brilliant Blue R on dye removal efficiency.

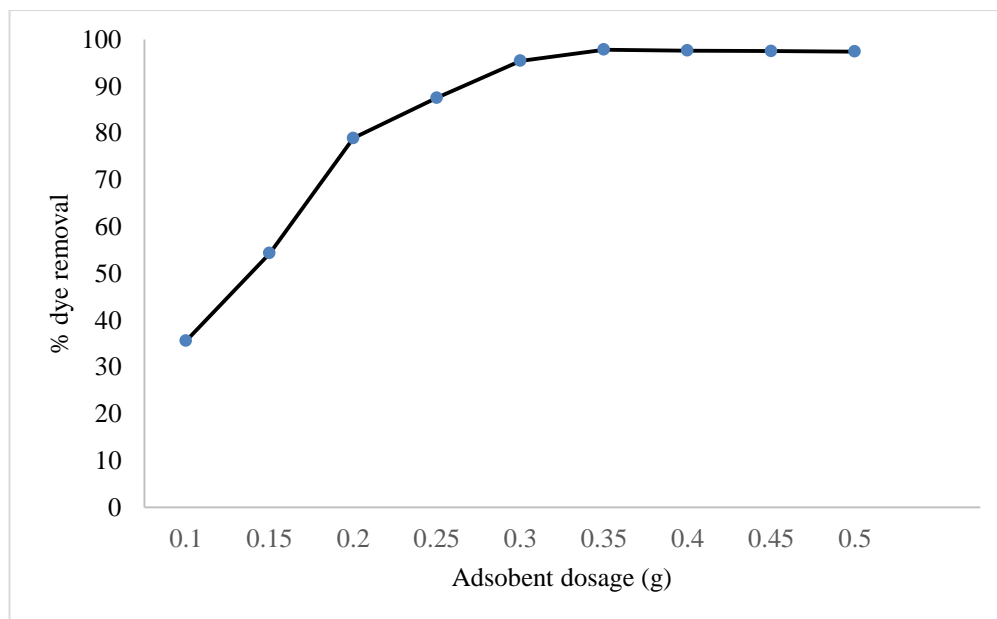


Figure-9: Adsorbent dosage effect on Reactive Brilliant Blue R.

Isotherm Studies: Adsorption isotherms for the deduction of dye (Reactive Brilliant Blue R) with the obtained Silver nanoparticles: The capacities of Silver nanoparticles for treating Reactive Brilliant Blue R were considered by testing the first and last concentration of the test solution. Various concentrations (10mg/L to 50mg/L) were tried having same adsorbent dosage of 300mg, at a neutral pH. Two model isotherms were handled to normalize the obtained adsorption data³². One model was assumed, that the adsorption of Reactive Brilliant Blue R occurs in monolayer in a uniform surface and is articulated as

$$\frac{C_e}{q_e} = \frac{1}{K_L \cdot q_m} + \frac{C_e}{q_m} \quad (3)$$

where K_L (L/mg) is the Langmuir equilibrium constant. It relates the affinity of the binding sites with the adsorbate.

q_m (mg/g) is the monolayer capability. It refers to the quantity of Reactive Brilliant Blue R needed to reside in all the accessible sites in one unit of sample.

Separation factor R_L displays the indication for bio sorbent interaction with the adsorbate and adsorbent.

The values obtained for Separation factor indicates if: $R_L > 1$ unfavorable interaction, $R_L = 1$ linear, favorable if $R_L < 0$ and the system is irretrievable if $R_L = 0$.

The Equation to find R_L : $R_L = 1 / (1 + K_L C_0)$ (4)

Table-1: Kinetic parameters for Langmuir and Freundlich.

q_m (mg/g)	Langmuir			Freundlich		
	K_L (l/mg)	R^2	R_L	K_F (1/min)	n	R^2
4.529	0.2744	0.9922	0.09	195.781	5.277	0.9809

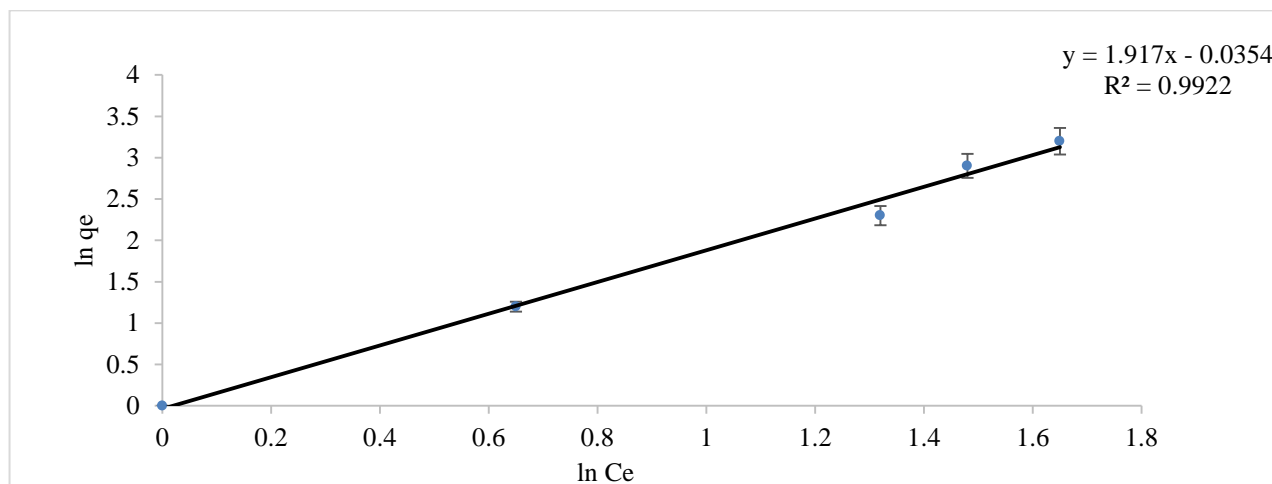


Figure-10: Concentration adsorption for the Freundlich isotherm.

The Freundlich expression is given as follows:

$$\ln q_e = \ln K_F + \left(\frac{1}{n}\right) \ln C_e \quad (5)$$

It is an equation relied on the adsorption onto diverse surface. K_F (mg/g) represents the Freundlich constant, the adsorption capacity and $1/n$, heterogeneity factor.

The values obtained from our results for Langmuir and Freundlich isotherm and the parameters obtained with correlation coefficient (R^2) are tabulated in Table-1.

Figures-10 and 11 show Freundlich and Langmuir models, respectively. The results for the parameters obtained are revealed in Table-1. From the data of the correlation coefficient in Table1 and Figures-10 and 11, it can be clear and evident that the obtained data of the adsorption is better for Langmuir model than that of Freundlich model³³. It is supported by the values of R^2 closer to unity, the linear correlation coefficients. The Value of R_L obtained superior than 1 shows the adsorption is favorable.

From the correlation coefficient data, it was very well obvious that Langmuir isotherm was very well fitted here. The constants K_L (L/mg) value was established at 0.2744L/mg and q_m established at 4.529mg/g. In Langmuir, there would have been higher diffusion into the pores due to mono layer diffusion. Since this attempt is the first for reactive dye adsorption with Silver nanoparticles, there is no evidence of proof for monolayer adsorption.

Effect of contact time on the adsorption of Reactive Brilliant Blue R: Contact time is a decisive factor for deciding the success of the adsorbent. It needs to be quick in adsorbing the dyes from real time effluent to give a significant result. The impact of the contact time on adsorption capacity, carrying capacity of the dye with the adsorbent was studied (Figure-12) Results confirm that a rapid adsorption of the Reactive Brilliant Blue R occurred within 3 min and reached an equilibrium value at 50 min for different concentration of the dye. The rapid biosorption of the dye within 3 min can be ascribed to the larger availability of active sites on Silver nanoparticles. As and when

the active sites are steadily occupied, the adsorption became saturated.

Kinetic on the removal of Reactive Brilliant Blue R: Kinetic models are thoroughly studied to know the controlling mechanism of the biosorption process which includes chemical reaction, diffusion and mass transfer.

Pseudo-first order and pseudo-second-order³⁴, which was commonly studied, are also studied in this work.

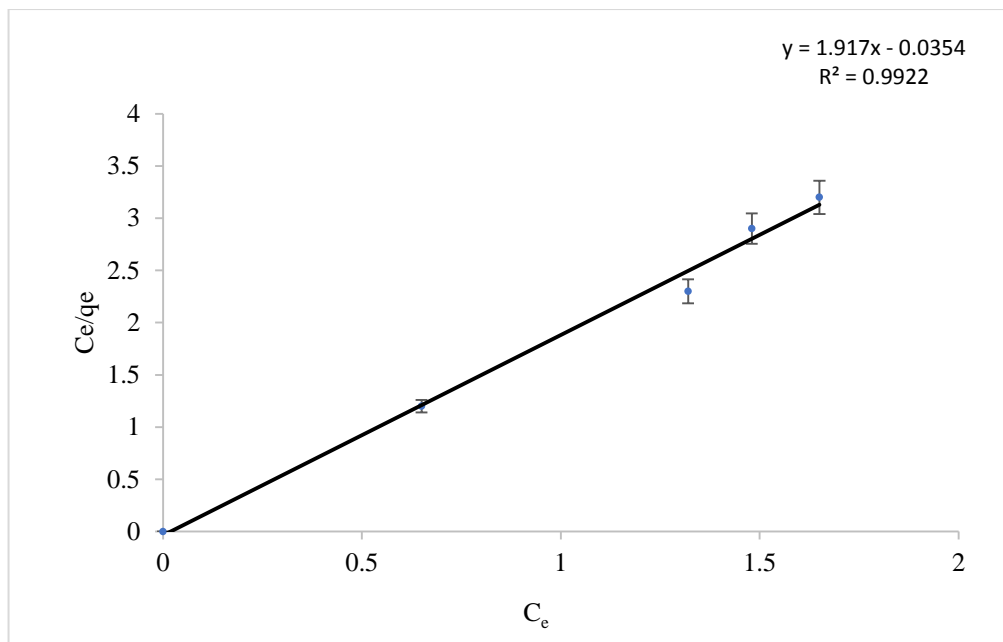


Figure-11: Concentration adsorption- Langmuir isotherm.

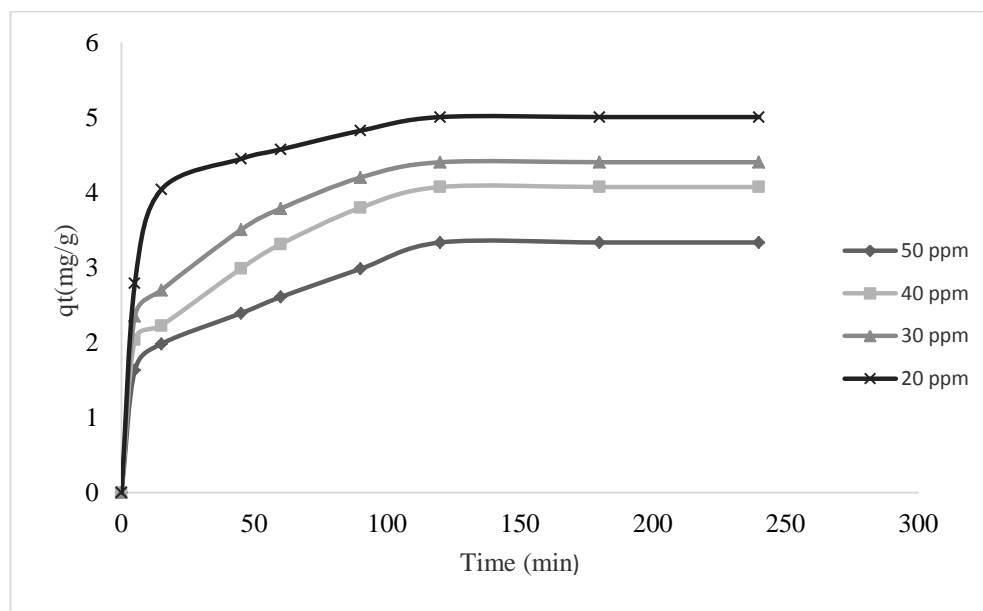


Figure-12: Adsorption capacities of Silver nanoparticles pertaining to time of contact and initial concentration of the dye.

When diffusion is the rate limiting step, pseudo-first-order model is considered that is as follows:

$$\ln(q_{e,exp} - q_t) = \ln q_{e,cal} - (k_1)t \quad (6)$$

k_1 (1/min): Rate constant for pseudo-first-order, $q_{e,exp}$: Equilibrium experiment adsorption capacity, $q_{e,cal}$: Equilibrium calculated adsorption capacity, q_t (mg/g): adsorption capacity at any time t .

The rate limiting step when pseudo-second order model supposes chemisorptions:

$$\frac{t}{q_t} = \frac{1}{k_2 q_e^2} + \frac{t}{q_e} \quad (7)$$

K_2 is rate constant (g/mg min)

By plotting $\ln(q_{e,exp} - q_t)$ versus t and (t/q_t) versus t ; respectively (Figure-13a and b), pseudo-first and pseudo-second order kinetic models are determined. The strength of each model was projected by estimated R^2 . Figure-13a and b, clearly indicates the best fit model, that is pseudo-second-order model.

From the relationship data R^2 values of pseudo-second-order model (0.999) was a lot quicker to one on comparison with pseudo-First-order model (0.945). Reactive Brilliant Blue R on the Silver nanoparticles was highly influenced by adsorption system through higher order kinetics. Also, the regularity between the experimental and theoretical values of equilibrium adsorption capacity (q_e) proved that the adsorption experiments are well in closer fitting through pseudo-second-order model once again.

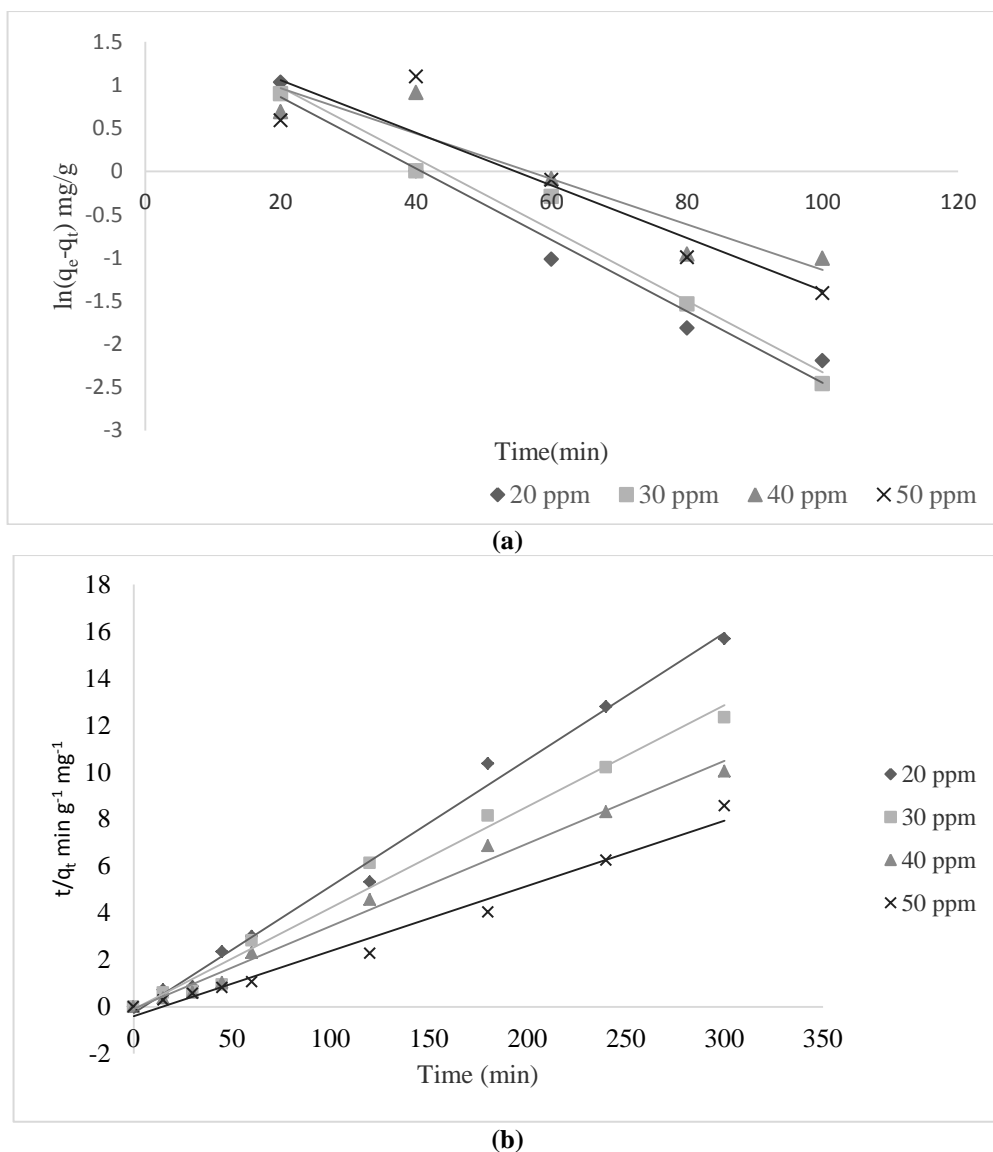


Figure-13: (a) Model kinetics of Pseudo-first order and (b) Model kinetics of Pseudo-second order.

Conclusion

In the current work, Silver nanoparticles obtained from *Tamarindus indica* leaf extract showed characteristic properties of the nanoparticles. A novel Silver nanoparticle was reported in this work. The FTIR analysis indicates the presence of hydroxyl and amine functional groups present on the nanoparticle surface which can be used for better surface fictionalization of the nanoparticles. These surface groups take a main part in increasing the adsorption capacity of the Silver nanoparticles. XRD studies confirmed that face centered cubic crystal structure for obtained silver nanoparticles with average crystallite size to be 18.4nm that matched with JCPDS reference no. 87-07020. The TEM image revealed the homogeneously distributed Silver nanoparticles size of around 20nm. Surface coatings seen in these images shows the capping of phytochemicals obtained from the *Tamarindus indica* leaf extract.

The adsorption of Reactive Brilliant Blue R onto Silver nanoparticles relied on pH variation. The optimum temperature for maximum adsorption of Reactive Brilliant Blue R was found out to be 27°C. The kinetics study revealed that the experimental data applies largely to pseudo-second order adsorption kinetics. Hence, chemisorption process is finalized as rate limiting step for this process. Also, the isotherm studies showed Langmuir adsorption behavior with monolayer homogeneous surface adsorption with highest adsorption capacity to be 5.3529 mg/g. Thus, the biologically synthesized silver nanoparticles can be employed to remove Reactive Brilliant Blue R.

References

1. Literathy P(1981)Industrial effluent treatment, vol. 1. Water and solid wastes: Edited By J. K. Walter and A. Wint. Applied Science Publishers Ltd, London. 1981. Pp. 351. ISBN 0 85334 981.https://doi.org/10.1016/0143-1471(82)90147-7
2. Mohamed A. Hassaan, Ahmed El Nemr.(2017) Health and Environmental Impacts of Dyes: Mini Review. Amer.Jl. of Env. Sci.and Engg.1 (3) 64-67. doi: 10.11648/j.ajese.20170103.11.
3. Chakraborty J.N. and Chakraborty J.N. (2015). Fundamentals and practices in colouration of textiles. CRC Press. pp.248ISBN 13: 9788190800143.
4. Lellis, B., Fávaro-Polonio, C. Z., Pamphile, J. A., & Polonio, J. C. (2019). Effects of textile dyes on health and the environment and bioremediation potential of living organisms. *Biotechnology Research and Innovation*, 3(2), 275-290. https://doi.org/10.1016/j.biori.2019.09.001https://doi.org/10.1016/j.biori.2019.09.001
5. Gogate, P. R., & Pandit, A. B. (2004). A review of imperative technologies for wastewater treatment II: Hybrid methods. *Advances in Environmental Research*, 8(3-4), 553-597. https://doi.org/10.1016/s1093-0191(03)00031-5
6. Nayantara, & Kaur, P. (2018). Biosynthesis of nanoparticles using eco-friendly factories and their role in plant pathogenicity: A review. *Biotechnology Research and Innovation*, 2(1), 63-73. https://doi.org/10.1016/j.biori.2018.09.003
7. McNamara, K., & Tofail, S. A. (2016). Nanoparticles in biomedical applications. *Advances in Physics: X*, 2(1), 54-88. https://doi.org/10.1080/23746149.2016.1254570
8. Thamilselvi, V., & Radha, K. V. (2017). Silver nanoparticle loaded silica adsorbent for wastewater treatment. *Korean Journal of Chemical Engineering*, 34(6), 1801-1812. https://doi.org/10.1007/s11814-017-0075-4
9. Jayakumar, A., & Vedhaiyan, R. K. (2019). Rapid synthesis of phytogetic silver nanoparticles using *Clerodendrum splendens*: Its antibacterial and antioxidant activities. *Korean Journal of Chemical Engineering*, 36(11), 1869-1881. https://doi.org/10.1007/s11814-019-0389-5
10. Anu Mary Ealia, S., & Saravanakumar, M. P. (2017). A review on the classification, characterisation, synthesis of nanoparticles and their application. *IOP Conference Series: Materials Science and Engineering*, 263, 032019. https://doi.org/10.1088/1757-899x/263/3/032019
11. Ruthven, D. M. (1984). Principles of adsorption and adsorption processes. John Wiley & Sons. pp.464ISBN: 978-0-471-86606-0
12. Tang, L., Zhang, S., Zeng, G., Zhang, Y., Yang, G., Chen, J., Wang, J., Wang, J., Zhou, Y., & Deng, Y. (2015). Rapid adsorption of 2,4-dichlorophenoxyacetic acid by iron oxide nanoparticles-doped carboxylic ordered mesoporous carbon. *Journal of Colloid and Interface Science*, 445, 1-8. https://doi.org/10.1016/j.jcis.2014.12.074
13. Escalona-Arranz, J., Péres-Roses, R., Urdaneta-Laffita, I., Camacho-Pozo, M., Rodríguez-Amado, J., & Licea-Jiménez, I. (2010). Antimicrobial activity of extracts from *Tamarindus indica* L. leaves. *Pharmacognosy Magazine*, 6(23), 242. https://doi.org/10.4103/0973-1296.66944
14. Sasidharan, S., Chen, Y., Saravanan, D., Sundram, K., & Latha, L. (2010). Extraction, isolation and characterization of Bioactive compounds from plants' extracts. *African Journal of Traditional, Complementary and Alternative Medicines*, 8(1). https://doi.org/10.4314/ajtcam.v8i1.60483
15. Ndikau, M., Noah, N. M., Andala, D. M., & Masika, E. (2017). Green synthesis and characterization of silver nanoparticles using *Citrullus lanatus* fruit rind extract. *International Journal of Analytical Chemistry*, 2017, 1-9. https://doi.org/10.1155/2017/8108504
16. Elamawi, R. M., Al-Harbi, R. E., & Hendi, A. A. (2018). Biosynthesis and characterization of silver nanoparticles using *Trichoderma longibrachiatum* and their effect on

- phytopathogenic fungi. *Egyptian Journal of Biological Pest Control*, 28(1). <https://doi.org/10.1186/s41938-018-0028-1>
17. Zhang, X., Liu, Z., Shen, W., & Gurunathan, S. (2016). Silver nanoparticles: Synthesis, characterization, properties, applications, and therapeutic approaches. *International Journal of Molecular Sciences*, 17(9), 1534. <https://doi.org/10.3390/ijms17091534>
 18. Chen, L., Liao, J., Chuang, Y., & Fu, Y. (2010). Characterization of crystalline silica nanorods synthesized via a solvothermal route using polyvinylbutyral as a template. *Journal of Nanoparticle Research*, 13(2), 783-790. <https://doi.org/10.1007/s11051-010-0078-0>
 19. Sasikumar, R., Ranganathan, P., Chen, S., Sireesha, P., Chen, T., Veerakumar, P., Rwei, S., & Kavitha, T. (2017). Economically applicable Ti₂O₃ decorated M-aMinophenol-forMaldehyde resin microspheres for dye-sensitized solar cells (DSSCs). *Journal of Colloid and Interface Science*, 494, 82-91. <https://doi.org/10.1016/j.jcis.2017.01.061>
 20. Premasudha, P., Venkataramana, M., Abirami, M., Vanathi, P., Krishna, K., & Rajendran, R. (2015). Biological synthesis and characterization of silver nanoparticles using *Eclipta alba* leaf extract and evaluation of its cytotoxic and antimicrobial potential. *Bulletin of Materials Science*, 38(4), 965-973. <https://doi.org/10.1007/s12034-015-0945-5>
 21. Burks, T., Avila, M., Akhtar, F., Göthelid, M., Lansåker, P., Toprak, M., Muhammed, M., & Uheida, A. (2014). Studies on the adsorption of chromium (VI) onto 3-Mercaptopropionic acid coated superparamagnetic iron oxide nanoparticles. *Journal of Colloid and Interface Science*, 425, 36-43. <https://doi.org/10.1016/j.jcis.2014.03.025>
 22. Durán, N., Marcato, P. D., Conti, R. D., Alves, O. L., Costa, F. T., & Brocchi, M. (2010). Potential use of silver nanoparticles on pathogenic bacteria, their toxicity and possible mechanisms of action. *Journal of the Brazilian Chemical Society*, 21(6), 949-959. <https://doi.org/10.1590/s0103-50532010000600002>
 23. Ho, Y., & McKay, G. (1999). Pseudo-second order model for sorption processes. *Process Biochemistry*, 34(5), 451-465. [https://doi.org/10.1016/s0032-9592\(98\)00112-5](https://doi.org/10.1016/s0032-9592(98)00112-5)
 24. Vinay, S. P. (2019). Green synthesis and characterization of silver nanoparticles using cassia *Auriculata* leaves extract and its efficacy as a potential antibacterial and cytotoxic effect. *Advanced Materials Letters*, 10(11), 844-849. <https://doi.org/10.5185/amlett.2019.0046>
 25. Siddiqi, K. S., Husen, A., & Rao, R. A. (2018). A review on biosynthesis of silver nanoparticles and their biocidal properties. *Journal of Nanobiotechnology*, 16(1). <https://doi.org/10.1186/s12951-018-0334-5>
 26. Gopalakrishnan, V., Radha, K. V., & Devasena, T. (2019). Silver nanoparticles synthesised using *Andrographis paniculata* ameliorates oxidative stress in erythrocyte model. *Materials Research Express*, 6(8), 0850b6. <https://doi.org/10.1088/2053-1591/ab24ea>
 27. Han, C., Han, J., Li, Q., & Xie, J. (2013). Wet chemical controllable synthesis of hematite ellipsoids with structurally enhanced visible light property. *The Scientific World Journal*, 2013, 1-5. <https://doi.org/10.1155/2013/410594>
 28. Jyoti, K., Baunthiyal, M., & Singh, A. (2016). Characterization of silver nanoparticles synthesized using *urtica dioica* Linn. leaves and their synergistic effects with antibiotics. *Journal of Radiation Research and Applied Sciences*, 9(3), 217-227. <https://doi.org/10.1016/j.jrras.2015.10.002>
 29. Anastopoulos, I., Robalds, A., Tran, H. N., Mitrogiannis, D., Giannakoudakis, D. A., Hosseini-Bandegharai, A., & Dotto, G. L. (2018). Removal of heavy metals by leaves-derived biosorbents. *Environmental Chemistry Letters*, 17(2), 755-766. <https://doi.org/10.1007/s10311-018-00829-x>
 30. Silva, F., Nascimento, L., Brito, M., Da Silva, K., Paschoal, W., & Fujiyama, R. (2019). Biosorption of methylene blue dye using natural Biosorbents made from weeds. *Materials*, 12(15), 2486. <https://doi.org/10.3390/ma12152486>
 31. Cardoso, N. F., Lima, E. C., Pinto, I. S., Amavisca, C. V., Royer, B., Pinto, R. B., Alencar, W. S., & Pereira, S. F. (2011). Application of cupuassu shell as bio sorbent for the removal of textile dyes from aqueous solution. *Journal of Environmental Management*, 92(4), 1237-1247. <https://doi.org/10.1016/j.jenvman.2010.12.010>
 32. Adeogun, A. I., Akande, J. A., Idowu, M. A., & Kareem, S. O. (2019). Magnetic tuned sorghum Husk biosorbent for effective removal of cationic dyes from aqueous solution: Isotherm, kinetics, thermodynamics and optimization studies. *Applied Water Science*, 9(7). <https://doi.org/10.1007/s13201-019-1037-2>
 33. Ahmad, M. A., Ahmad, N., & Bello, O. S. (2015). Removal of Remazol brilliant blue reactive dye from aqueous solutions using watermelon rinds as adsorbent. *Journal of Dispersion Science and Technology*, 36(6), 845-858. <https://doi.org/10.1080/01932691.2014.925400>
 34. Jarusiripot, C. (2014). Removal of reactive dye by adsorption over chemical Pretreatment coal-based bottom ash. *Procedia Chemistry*, 9, 121-130. <https://doi.org/10.1016/j.proche.2014.05.015>